MOLECULAR AND CELLULAR BIOLOGY, Apr. 1988, p. 1558–1569
0270-7306/88/041558-12$02.00/0

Vol. 8, No. 4

Exploitation of a Thermosensitive Splicing Event To Study Pre-mRNA Splicing In Vivo

PAUL E. CIZDZIEL, MARYELLEN DE MARS, AND EDWIN C. MURPHY, JR.*

Department of Tumor Biology, Section of Virology, The University of Texas System Cancer Center, M. D. Anderson Hospital and Tumor Institute, Houston, Texas 77030

Received 6 July 1987/Accepted 8 January 1988

The spliced form of MuSVts110 viral RNA is approximately 20-fold more abundant at growth temperatures of 33°C or lower than at 37 to 41°C. This difference is due to changes in the efficiency of MuSVts110 RNA splicing rather than selective thermolability of the spliced species at 37 to 41°C or general thermosensitivity of RNA splicing in MuSVts110-infected cells. Moreover, RNA transcribed from MuSVts110 DNA introduced into a variety of cell lines is spliced in a temperature-sensitive fashion, suggesting that the structure of the viral RNA controls the efficiency of the event. We exploited this novel splicing event to study the cleavage and ligation events during splicing in vivo. No spliced viral mRNA or splicing intermediates were observed in MuSVts110-infected cells (6m2 cells) at 39°C. However, after a short (about 30-min) lag following a shift to 33°C, viral pre-mRNA cleaved at the 5′ splice site began to accumulate. Ligated exons were not detected until about 60 min following the initial detection of cleavage at the 5′ splice site, suggesting that these two splicing reactions did not occur concurrently. Splicing of viral RNA in the MuSVts110 revertant 54-5A4, which lacks the sequence -AG/TGT- at the usual 3′ splice site, was studied. Cleavage at the 5′ splice site in the revertant viral RNA proceeded in a temperature-sensitive fashion. No novel cryptic 3′ splice sites were activated; however, splicing at an alternate upstream 3′ splice site used at low efficiency in normal MuSVts110 RNA was increased to a level close to that of 5′-splice-site cleavage in the revertant viral RNA. Increased splicing at this site in 54-5A4 viral RNA is probably driven by the unavailability of the usual 3′ splice site for exon ligation. The thermosensitivity of this alternate splice event suggests that the sequences governing the thermodependence of MuSVts110 RNA splicing do not involve any particular 3′ splice site or branch point sequence, but rather lie near the 5′ end of the intron.

Previous studies from this laboratory have determined the basis for the temperature-sensitive phenotype displayed by NRK cells infected with the mutant MuSVts110 retrovirus (6m2 cells). MuSVts110 originated from wild-type murine sarcoma virus (MuSV) as the result of a 1,487-base central deletion between nucleotides 2404 in the 3′ end of the p30 region and 3892 in the 5′ end of the v-*mos* gene (22, 23). (Previous reports [22] erroneously indicated that the deletion in MuSVts110 DNA relative to wild-type MuSV-124 was 1,488 bases in length.) The junction of the *gag* and *mos* genes is out of frame and contains two in-frame translational terminators just downstream of the junction point (22, 23). Thus, the 3.8-kilobase (kb) MuSVts110 transcript can be translated into a truncated *gag* gene precursor, $P58^{gag}$, only (11). (In a number of previous studies [5, 8, 11, 22, 23, 32], the MuSVts110 RNAs were estimated to be 4.0 and 3.5 kb in size. Precise definition of the deletion boundaries and splice sites [23] indicates that the unspliced and spliced MuSVts110 RNAs are actually 3.8 and 3.3 kb in size, respectively.) At 39°C, this 3.8-kb RNA is not spliced and 6m2 cells appear morphologically normal (4, 11). However, at growth temperatures of 33°C or lower, a 431-base intron surrounding the *gag-mos* junction can be removed (22). The reorganized viral transcript, 3.3 kb in length, contains the *gag* and *mos* genes in a continuous open reading frame that is translated to yield $P85^{gag\text{-}mos}$, a serine kinase capable of transforming cells (15, 16).

Our objectives in the current work were to define the basis for the accumulation of the spliced transcript at low growth temperatures and to exploit, if possible, the novel splicing event to study the molecular events occurring during splicing of this RNA in vivo. We found that the amount of spliced viral RNA produced was determined by splicing efficiency rather than by any selective instability of the spliced RNA at higher growth temperatures or any general thermosensitivity of RNA splicing in MuSVts110-infected cells. Moreover, we determined by transfection of a MuSVts110 DNA into a variety of cell lines that the structure of the viral transcript was the primary determinant governing the splice event.

The kinetics of the cleavage and ligation events occurring during the splicing of the MuSVts110 transcript were also determined. In HeLa cell nuclear extracts, splicing of presynthesized mRNA precursors occurs through an orderly series of cleavage and ligation events. A series of recent studies have established that the first step after spliceosome formation is cleavage at the 5′ splice site and the concurrent formation of a branched intermediate. In the second step, the exons are ligated and the branch-point-containing intron is released (reviewed in references 7, 20, and 25). Analyses of steady-state levels of beta-globin RNA splicing intermediates in cells have confirmed this model (35), but in only one case has a mammalian pre-mRNA been observed through the splicing process in vivo (36). Following a shift to a growth temperature permissive for splicing in MuSVts110-infected cells, it was possible to monitor the kinetics of 5′ splice site cleavage and exon ligation.

In MuSVts110 revertant viral RNA lacking the AG dinucleotide at the usual 3′ splice site, the 5′ splice site was spliced to an alternate 3′ splice site used inefficiently in normal MuSVts110 transcripts. No cryptic sites near the

* Corresponding author.

usual 3′ splice site were recruited. Moreover, this alternate splicing of the revertant RNA occurred only at growth temperatures normally permissive for splicing of the authentic MuSVts110 RNA, suggesting that temperature-sensitive splicing was determined by sequences at the 5′ end of the MuSVts110 and was independent of the particular 3′ splice site or branch point used.

MATERIALS AND METHODS

Cell lines. NRK cells infected with MuSVts110 (6m2 cells) characteristically appear morphologically transformed at 33°C and normal at 39°C. Additionally, 6m2 cells readily form colonies in soft agar at 33°C but not at 39°C (3). The revertant 54-5A4 cell line was derived from a clone of parental MuSVts110-nonproducer 6m2 cells that spontaneously acquired the ability to grow in soft agar at both 39 and 33°C. This cell line was maintained at 37°C in McCoy medium containing 10% fetal calf serum. The 6m2 cell line was maintained in the same medium at 33°C. NIH 3T3 cells were maintained in Dulbecco high-glucose medium supplemented with 10% fetal calf serum.

For temperature shift experiments, 6m2 cells were grown at 33°C and then incubated at 39°C overnight. Rapid shifts from 39 to 33°C were done by replacing the 39°C medium in a culture with fresh medium equilibrated at 33°C and immediately immersing the culture in a 33°C water bath. Shifts from 33 to 39°C were done in exactly the same manner with the medium and water bath at 39°C.

DNA probes used in S1 analyses. The DNA probes used in S1 analyses were originally described by Nash et al. (23) and are briefly described here for clarity.

(i) pBA.36. pBA.36 is a 356-base-pair fragment of MuSV-124 DNA (34) that extends from a *Bgl*II site at nucleotide 3698 across both the *gag/mos* junction point and the 3′ splice site in MuSVts110 RNA to an *Ava*I site at nucleotide 4056 (Fig. 1). The unspliced MuSVts110 viral RNA will protect 175 bases of this DNA from S1 nuclease, whereas the spliced 3.3-kb RNA will protect only 122 bases.

(ii) DD.29. DD.29 is a 290-base-pair fragment of the pMLV-1 *gag* gene (31) that extends from a *Dde*I site at nucleotide 1481 across the 5′ splice site utilized in MuSVts110 to a *Dde*I site at nucleotide 1771 (Fig. 1), corresponding to nucleotides 1902 to 2192 in the MuSV-124 sequence (34). Unspliced MuSVts110 RNA will protect all 290 bases of DD.29 from S1 nuclease; the spliced viral transcript will protect only 120 bases.

(iii) SX1.1. SX1.1 was constructed from the MuSVts110 equivalent DNA (see Fig. 5) and extends from an *Xmn*I site 137 bases downstream of the 3′ splice site to an *Xho*I site 35 bases upstream of the 5′ splice site (Fig. 1). Unspliced MuSVts110 RNA will protect 602 bases of the probe; the spliced RNA will protect only 137 bases.

(iv) pXX.441. pXX.441 is a 441-base-pair fragment of murine leukemia virus (MuLV) DNA extending from an *Xba*I site at nucleotide 5326 to another *Xba*I site at nucleotide 5767 (31) subcloned into the pT7/T3-18 vector (Bethesda Research Laboratories, Inc.). Full-length MuLV RNA will protect all 441 bases of the insert from S1 nuclease; spliced MuLV *env* RNA will protect either 276 or 290 bases of pXX.441, depending on which of the reported 3′ splice sites (19, 21) are used.

(v) BB.220. BB.220 is a 220-base DNA fragment obtained from the MuSVts110 equivalent DNA (see Fig. 5), which extends from a *Bst*NI site at nucleotide 2220 to another *Bst*NI site at nucleotide 2421, 26 bases upstream of the MuSVts110 3′ splice site. Unspliced MuSVts110 RNA will protect all 220 bases of 5′-end-labeled BB.220 from S1 nuclease. Viral RNA spliced at the MuSVts110 5′ and 3′ splice sites will fail to protect any of this probe, since it lies entirely within the intron. Revertant 54-5A4 viral DNA mutated at the 3′ splice site will also protect all of BB.220.

(vi) XN.369. XN.369 is a 369-base DNA fragment obtained from the MuSVts110 equivalent DNA (see Fig. 6), which extends from the *Xho*I site at nucleotide 1982 across the 5′ splice site to an *Nci*I site at nucleotide 2351. Unspliced MuSVts110 RNA will protect all 369 bases of 5′-end-labeled XN.369. Spliced viral RNA will not protect any of 5′-end-labeled XN.369. Revertant 54-5A4 viral RNA cleaved at the 5′ splice site will protect 334 bases of XN.369.

Construction of an equivalent of MuSVts110 DNA. To test the role of the 1,487 bases deleted from wild-type MuSV-349 (MuSV-124) DNA (nucleotides 2405 to 3891) (22) in generating the novel properties displayed by MuSVts110, we constructed an equivalent of MuSVts110 DNA by combining wild-type MuSV-124 DNA fragments from nucleotides 1 to 2351 and 3909 to 5833 with a synthetic junction oligonucleotide composed of nucleotides 2352 to 2404 joined to nucleotides 3892 to 3908 (see Fig. 5) (M. de Mars, P. E. Cizdziel, and E. C. Murphy, Jr., J. Virol., in press).

Purification of plasmid DNA. The various inserts and fragments described in the previous section were excised by digestion with the appropriate restriction enzyme(s), size fractionated on an 0.8% agarose gel, and stained with ethidium bromide. DNA was purified from the agarose by electroelution in TE buffer (10 mM Tris [pH 8], 10 mM EDTA). Electroeluted DNA fragments were further purified by chromatography on a NACS column (Bethesda Research Laboratories) as specified by the supplier.

In cases when small DNA fragments were purified from polyacrylamide gels, gel slices were crushed to a paste in 10 ml of TNE buffer (10 mM Tris [pH 8], 100 mM NaCl, 10 mM EDTA) and agitated overnight at 37°C. Acrylamide granules were removed by centrifugation, and DNA was purified from the supernatants by chromatography on a NACS column (Bethesda Research Laboratories).

RNA isolation. Total cellular RNA was isolated by guanidine thiocyanate extraction. Confluent monolayers of cells were first rinsed in A3 buffer (20 mM Tris [pH 7.5], 130 mM KCl, 5 mM magnesium acetate) and then directly lysed with 8 ml of prechilled 4 M guanidine thiocyanate–0.5% sodium sarcosyl–25 mM sodium citrate (pH 7.0)–0.1 mM 2-mercaptoethanol per T-150 flask. The suspension was subjected to Dounce homogenization, layered over a 5.7 M CsCl cushion containing 100 mM EDTA [pH 7.0], and centrifuged in a Beckman SW41 rotor at 39,000 rpm at 18°C for 12 to 18 h. The supernatant was removed by aspiration, and the pellet

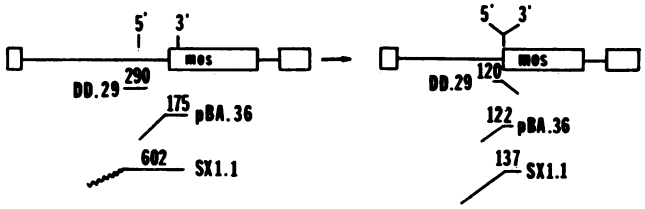

FIG. 1. Probes used for S1 nuclease analysis. The structures of the 3.8-kb unspliced (left) and 3.5-kb spliced (right) MuSVts110 RNAs are shown diagramatically. Underneath the 5′ and 3′ splice sites are shown the probes used for S1 nuclease analysis (DD.29, pBA.36, and SX1.1). The extent (in bases) to which each probe is protected by the viral RNA from S1 nuclease digestion is indicated.

was dried and dissolved in 3.0 ml of TE buffer. The solution was extracted with an equal volume of phenol-chloroform (1:1, vol/vol) and then with chloroform only; it was then precipitated with 0.1 volume of 4 M lithium acetate plus 2.5 volumes of 95% ethanol. The RNA was pelleted, dissolved in TE buffer, and stored at −70°C.

S1 nuclease analysis. DNA probes for S1 nuclease analysis were either 3′ or 5′ end-labeled as described previously (22, 23). Hybridization of cellular RNA with these probes and determination of viral gene expression by S1 nuclease analysis were performed as described previously (22, 23).

Quantitation of splicing intermediates. Unspliced RNA, splicing intermediates, and spliced RNA were quantitated by scanning the S1 nuclease gel profiles on a Beckman DU-8 spectrophotometer equipped with a scanner.

Measurement of viral RNA half-lives. 6m2 cells were seeded in T-25 flasks and grown to approximately 75% confluence at 33°C. Where indicated, actinomycin D (act D) (Sigma Chemical Co.) was added to 10 μg/ml, and the cells were further incubated at either 33 or 39°C for up to 24 h. RNA was prepared as described above from individual cultures at times indicated below, and all of the RNA from each culture was hybridized to 5′-end-labeled pBA.36 DNA and subjected to S1 analysis. The S1 gel profiles were scanned by using a Beckman DU-8 spectrophotometer, and the results are plotted as the $\log_2$ of the amount of the total viral RNA represented by each RNA species at the various time points.

RESULTS

Growth-temperature-dependent accumulation of the spliced MuSVts110 3.3-kb RNA. We have previously shown that 6m2 cells contain a single integrated copy of MuSVts110 DNA (5, 23), suggesting that both the 3.8- and 3.3-kb MuSVts110 RNAs are the products of a single gene and that the restriction of 3.3-kb RNA production to lower growth temperatures must reflect some posttranscriptional event. In addition, sequence analysis of these RNAs has shown that they are identical, except for a 431-base intron found in the larger RNA (22), making it very likely that the 3.3-kb RNA is a product of a thermosensitive RNA splicing event (13, 22).

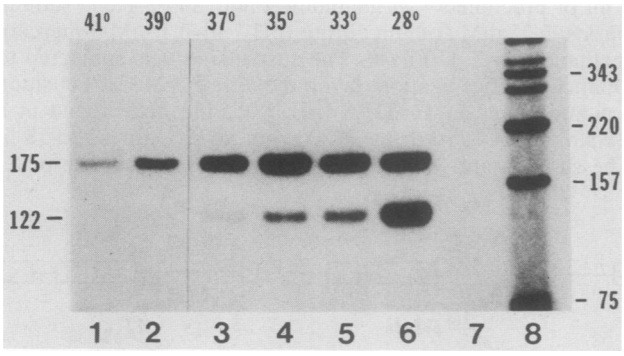

FIG. 2. Accumulation of the spliced MuSVts110 RNA as a function of growth temperature. Total cellular RNA (10 μg) from 6m2 cells grown at 28, 33, 35, 37, 39, and 41°C was hybridized to the 5′-end-labeled pBA.36 probe (Fig. 1). The hybrids were digested with S1 nuclease, and the protected fragments were analyzed on a 5% acrylamide gel containing 8 M urea. Lanes: 1 to 6, protection of pBA.36 by 6m2 RNA isolated from cells at 41 to 28°C, respectively; 7, pBA.36 probe-only control; 8, 5′-end-labeled pBR322 DNA-*Hin*fI digest.

TABLE 1. Steady-state levels of MuSVts110 RNAs as a function of growth temperature

Temp (°C)	Total amt of viral RNA[a]	Amt (%) of 3.8-kb RNA[a]	Amt (%) of 3.3-kb RNA[a]
28	18.5	8.0 (43)	10.5 (56)
33	10.6	8.0 (75)	2.6 (25)
35	11.5	9.4 (81)	2.1 (18)
37	6.3	5.9 (93.5)	0.4 (6.5)
39	3.1	3.0 (97.5)	0.08 (2.6)
41	1.2	1.1 (96.8)	0.04 (3.2)

[a] RNA quantities (expressed in arbitrary units) were estimated by scanning the S1 nuclease gel profile in Fig. 2. The amount of 3.8- and 3.3-kb RNAs present at each growth temperature was inferred from the levels of the pBA.36 175- and 122-base protection fragments, respectively.

Our previous data favored the interpretation that the MuSVts110 3.8-kb RNA is transcribed at all growth temperatures but can be spliced only at 33°C or lower. However, it was possible that efficient splicing occurred at all growth temperatures and that the absence of the 3.3-kb RNA at 39°C might reflect a high degree of instability at this temperature rather than a failure to be produced. Additionally, it was considered possible, although unlikely, that thermosensitivity was a general feature of pre-mRNA splicing in 6m2 cells. To explore these possibilities, we examined the splicing and stability of MuSVts110 RNA at various growth temperatures and tested the specificity of the thermosensitive splicing event.

To measure the growth temperature dependence of MuSVts110 RNA accumulation, RNA from 6m2 cells grown at 33°C and then shifted to a variety of temperatures between 28 and 41°C was analyzed for 3.8- and 3.3-kb viral RNA production by S1 nuclease analysis with the 3′-splice-site-specific probe pBA.36 (Fig. 1). The S1 nuclease results were quantitated by scanning the gel profiles. As estimated by the protection of the 175-base fragment of pBA.36, the MuSVts110 3.8-kb RNA was transcribed to various extents at all growth temperatures (Fig. 2, lanes 1 to 6; Table 1). Steady-state levels of the 3.8-kb RNA were highest at 28 to 37°C (Fig. 2, lanes 3 to 6; Table 1) and were reduced two- to threefold at 39 to 41°C (Fig. 2, lanes 1 and 2; Table 1). The proportion of spliced 3.3-kb MuSVts110 RNA, as estimated from the 122-base protection fragment, was high (56%) at 28°C, substantial (18 to 25%) at 33 to 35°C, and barely detectable (2 to 3%) at 39 to 41°C (Fig. 2, lanes 1 to 6; Table 1). At the extremes of the temperature range (28 and 39°C), there was an approximately 20-fold difference in the production of spliced MuSVts110 RNA (Table 1).

Specificity of thermosensitive MuSVts110 RNA splicing. To test whether other pre-mRNAs in 6m2 cells might also exhibit restricted splicing, we measured the efficiency of MuLV envelope mRNA splicing in superinfected 6m2 cells as a function of growth temperature. Splicing of the MuLV *env* mRNA was measured by S1 nuclease analysis with a probe (pXX.441) that extended across both of the potential *env* gene 3′ splice sites (Fig. 3A). Unspliced MuLV RNA was expected to protect 441 bases of pXX.441; spliced *env* mRNA should protect either 276 or 290 bases depending on which *env* gene 3′ splice site (19, 21) was used. As estimated from the protection of a nearly constant level of a 290-base fragment across the entire temperature range tested (Fig. 3B, lanes 1 to 6), splicing of the MuLV *env* mRNA was judged to be temperature independent. A quantitative estimate (not shown) of MuLV transcription and splicing efficiency was obtained by scanning the gel profiles shown in Fig. 3B. Using

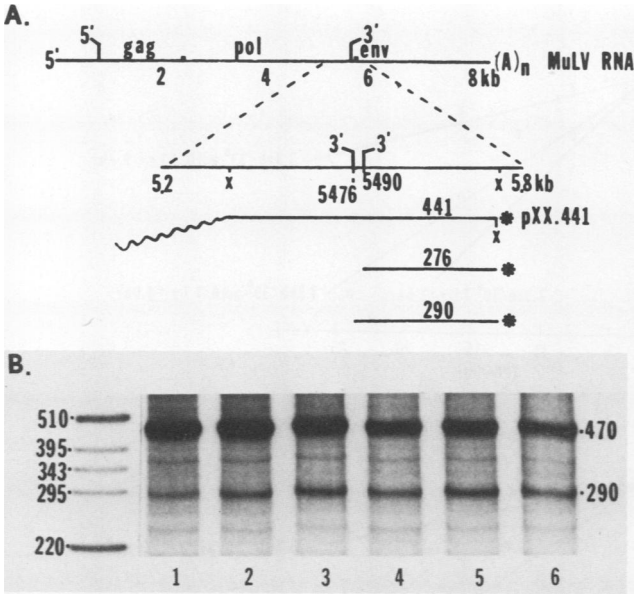

FIG. 3. Splicing of MuLV *env* mRNA as a function of growth temperature. RNA was obtained from MuLV-superinfected 6m2 cells grown at 33°C and shifted to 28, 35, 37, 39, or 41°C overnight. (A) Each RNA preparation (10 μg) was hybridized to the 3'-end-labeled MuLV *env* gene 3' splice site probe pXX.441. The hybrids were digested with S1 nuclease, and the protected fragments were analyzed on a 5% polyacrylamide gel containing 8 M urea. (B) Protection of pXX.441 by RNA from superinfected 6m2 cells grown at 28°C (lane 1), 33°C (lane 2), 35°C (lane 3), 37°C (lane 4), 39°C (lane 5), and 41°C (lane 6).

the extremes of the temperature range tested (28 and 41°C) as an example, quantitation showed that although total MuLV RNA levels decreased by 32% from 28 to 41°C, the percentage of MuLV RNA spliced remained relatively constant (27% at 28°C and 32% at 41°C). From these results, the thermosensitivity of the accumulation of MuSVts110 spliced RNA seems to be specific to that particular mRNA and not a general feature of the accumulation of spliced RNA species in 6m2 cells.

Stability of the spliced MuSVts110 RNA. To examine the possibility that the MuSVts110 3.3-kb RNA is constitutively produced but rapidly degraded at higher growth temperatures, thus explaining its nearly complete absence from 6m2 cells at 37 to 41°C, we compared its turnover at 33 and 39°C. Individual 6m2 cultures, grown initially at 33°C, were treated with 10 μg of actinomycin D (act D) per ml or left untreated and shifted to 33 or 39°C for up to 24 h. RNA prepared at various time points was subjected to S1 nuclease analysis with the pBA.36 probe (Fig. 4A). At 33°C in the presence of act D (Fig. 4A, top panel), the 3.3-kb viral RNA decayed with a half-life of 9.7 h, whereas the 3.8-kb RNA turned over more slowly, with a half-life of 19 h (compare Fig. 4B, upper and lower panels). Under these conditions, no new 3.8-kb RNA could be transcribed, but splicing was presumed to occur. Thus, the half-life calculated for the 3.8-kb RNA was probably an underestimate, and that of the 3.3-kb RNA was probably an overestimate. At 39°C in the presence of act D (Fig. 4A, middle panel), the decay rates for both viral RNAs were about twice as rapid as those observed at 33°C. Under these conditions, in which no transcription or splicing was expected to occur, the half-lives of the 3.3- and 3.8-kb RNAs were estimated to be 4 and 10 h, respectively (compare Fig. 4B, upper and lower panels). S1 nuclease analysis of 3.3-kb RNA decay at 39°C in the absence of act D (Fig. 4A, bottom panel) gave an estimated half-life of 3.5 h (Fig. 4B, upper panel), essentially identical to the 4-h half-life observed in the presence of the drug. We interpret these data as arguing that the 3.3-kb MuSVts110 RNA is not selectively thermolabile at 39°C. At 39°C, the half-life of the 3.3-kb RNA was decreased from about 10 to 4 h, whereas the half-life of the 3.8-kb RNA was similarly shortened from 19 to 10 h. Thus, the increased decay of the 3.3-kb RNA at 39°C is not selective, and hence the 10- to 20-fold reduction in the ratio of 3.3-kb to 3.8-kb viral RNA at 39°C over that observed at permissive temperatures (Table 1) cannot be explained by accelerated decay.

***cis*-Acting nature of the MuSVts110 splicing defect.** To ask whether the thermal defect in MuSVts110 RNA splicing was virus or cell specific, we constructed an MuSVts110 equivalent DNA from wild-type MuSV-124 DNA fragments and a synthetic oligonucleotide representing the *gag* gene-*mos* gene junction in MuSVts110 (Fig. 5; de Mars et al., in press). This construct contains the identical 1,487-base deletion found in MuSVts110 relative to wild-type MuSV-124. The equivalent MuSVts110 DNA (termed ts32 DNA) was transfected into Psi-2 and NIH 3T3 cells. In addition, NRK cells were infected with virus released from Psi-2/ts32 transfectants. In each case, these cells displayed a temperature-sensitive phenotype and produced a $P85^{gag\text{-}mos}$ kinase (de Mars et al., in press). Most importantly, viral RNA splicing in these cells was restricted to lower growth temperatures. As was the case with MuSVts110 RNA splicing in 6m2 cells (Fig. 6, lanes 3 to 6), splicing of the viral transcript in NIH 3T3 cells transfected with the ts32 DNA was readily observed at 28 and 33°C (lanes 7 and 8), but was reduced to trace levels at 37 to 41°C (lanes 9 and 10). A quantitative estimate of the relative levels of the ts32 transcripts was obtained by scanning the gel profile shown in Fig. 6. The spliced transcript was produced sixfold more efficiently at 33°C (lane 8) than at 41°C (lane 10). These data suggest strongly that thermosensitive splicing of the viral transcript is not governed by any altered component of the cellular splicing apparatus, but rather is specified by the structure of the RNA itself.

Cleavage and ligation events in MuSVts110 RNA splicing in vivo. To determine the kinetics of MusVts110 splicing in vivo, we depleted the 6m2 cells of all viral splicing intermediates and products by an overnight incubation at 41°C (22, 23). The cells were then shifted to 33°C, and cellular RNA was prepared at 20- to 30-min intervals over 6 h. The kinetics of 5'-splice-site cleavage and exon ligation were then measured by using a series of specific S1 nuclease reagents.

(i) 5'-Splice-site cleavage. In RNA from 6m2 cells shifted to 33°C for various times, cleavage at the 5' splice site, as estimated by the appearance of the 120-base protection fragment of the DD.29 probe (Fig. 1), was first detected visually at approximately 60 min following the shift (Fig. 7, lane 4). The cleavage products and ligated exons accumulated over the next several hours (Fig. 7, lanes 5 to 9).

(ii) Exon ligation. To determine the kinetics of the appearance of ligated exons relative to cleavage at the 5' splice site, two 3'-splice-site-specific probes, pBA.36 and SX1.1 (Fig. 1), were used to analyze the same RNA fractions. Protection of the 122-base fragment of pBA.36, characteristic of the ligated exons, was first detected visually at about 90 min following the shift to 33°C, approximately 30 min after cleavage at the 5' splice site was first noted (Fig. 8A, lane 5). Similarly, the 137-base protection fragment of SX1.1 was first observed at 100 min following the shift (Fig. 8B, 100-min

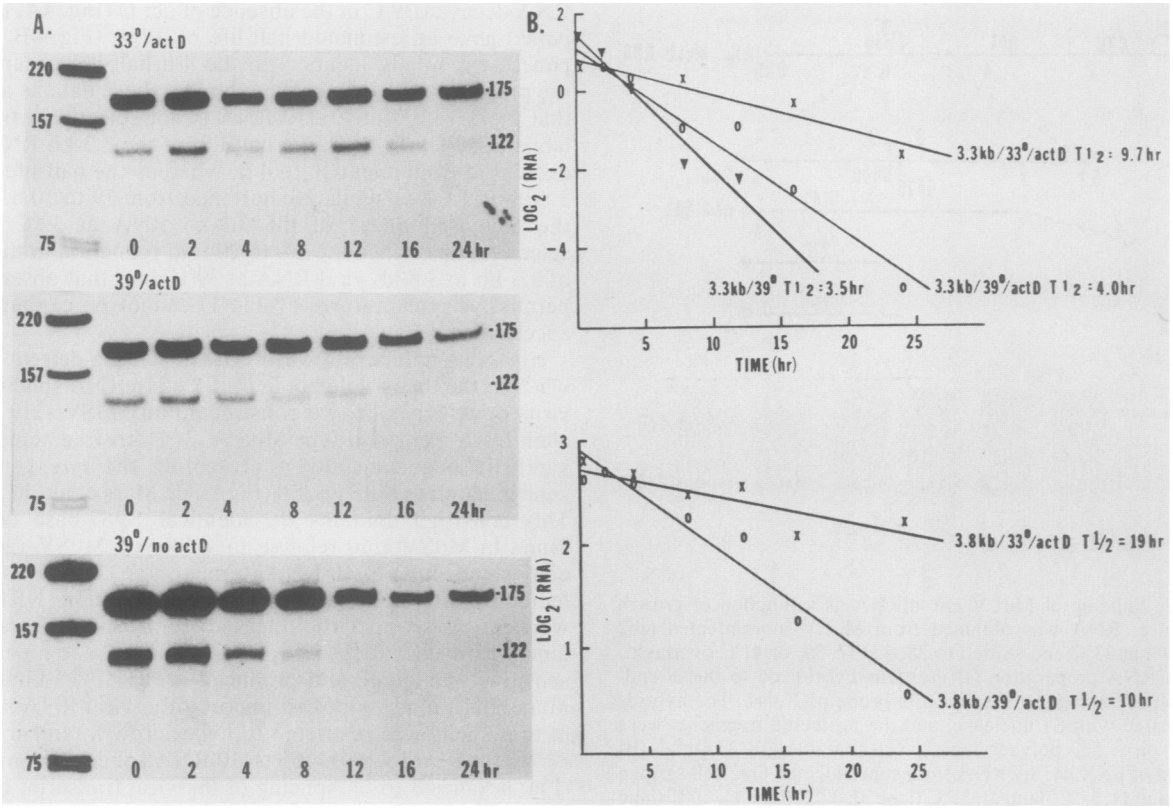

FIG. 4. MuSVts110 RNA half-life. Total cellular RNA was isolated from T-25 cultures of 6m2 cells grown at 33°C, treated with 10 μg of act D per ml or left untreated, and then grown at 33 or 39°C for various periods up to 24 h. A pBA.36 S1 nuclease assay was performed on the individual RNA preparations (all of the RNA isolated from a T-25 flask) to measure the extent of exon ligation. The 175- and 122-base protection fragments were quantitated by scanning the S1 nuclease gel profiles. (A) S1 nuclease analysis of RNA from 6m2 cells treated with act D and incubated at 33°C for 0, 2, 4, 8, 12, 16, or 24 h (top panel), treated with act D and incubated at 39°C for 0 to 24 h (middle panel), or not treated with act D and incubated at 39°C for 0 to 24 h (bottom panel). (B) Estimates of MuSVts110 RNA half-lives. The quantities of protection fragments seen in panel A were converted to $\log_2$ and plotted as $\log_2$ RNA versus time. The upper graph shows the half-life of the 3.3-kb MuSVts110 RNA at 33 and 39°C in the presence of act D and at 39°C in the absence of act D; the lower graph shows the half-life of the 3.8-kb MuSVts110 RNA at 33 and 39°C in the presence of act D.

lane). Thereafter, ligated exons accumulated at an approximately linear rate (Fig. 8A, lanes 5 to 9; to Fig. 8B, 120-min to 6-h lanes).

A quantitative estimate of the kinetics of the accumulation of MuSVts110 RNA splicing intermediates was obtained by scanning the gel profiles shown in Fig. 7 and 8. For each time point, the amount of viral RNA cleaved at the 5′ splice site or the amount of ligated exons was expressed as a fraction of the total MuSVts110 RNA detected (Fig. 9). The levels of the 120-base DD.29 protection fragment characteristic of 5′-splice-site cleavage represented well below 1% of the total viral RNA detected during the first 30 min after the shift from 39 to 33°C. Between 30 and 60 min after the shift there was an increase in the 120-base protection fragment to about 4.5% of the total viral RNA, after which the proportion of this fragment increased with nearly linear kinetics through 8 h. The proportion of ligated exons, as estimated by the levels of the 122-base pBA.36 or 137-base SX1.1 protection fragments, remained low and constant for the first 80 min after the shift, representing about 2% of the total viral RNA. After the 80-min time point, however, ligated exons appeared and then accumulated at approximately the same rate as cleaved 5′ splice sites.

Analyzed in this way, our results indicated that there was a somewhat greater than 30-min lag period after a shift to splicing-permissive conditions before the first splicing reactions could be detected. Cleavage at the 5′ splice site was first detected between 30 and 60 min after a shift to 33°C (Fig. 9, compare the 30- and 60-min time points). Regression analysis of the kinetics of accumulation of cleaved intermediates, however, suggested a shorter lag period, in the neighborhood of 6 min, prior to the initiation of 5′-splice-site cleavage (Fig. 9, inset). Thus, a precise estimate of the time required to initiate cleavage reactions in vivo after a shift to permissive conditions was not possible. The discrepancy between the 6-min and 30- to 60-min estimates, however, may reflect the time between which 5′-splice-site cleavage first occurs and the time at which sufficient levels of cleaved intermediates have accumulated to be detected. A similar rationale can be used to explain the discrepancy in times reported for the onset of exon ligation. Although regression analysis predicted the onset of exon ligation to occur about 67 min after a shift to 33°C (Fig. 9, inset), the MuSVts110 spliced RNA species could not be detected by S1 nuclease analysis until 80 to 100 min following the shift (Fig. 9, 80- to 100-min time points). Although it is not possible to determine the absolute times after a shift at which 5′-splice-site cleavage and exon ligation occurred, both analyses agreed that ligated exons were initially detected about 60 min after 5′-splice-site cleavage. Thus, although the time required to initiate splicing after a shift to 33°C cannot be exactly defined from our data, it seems very probable that 5′-splice-site

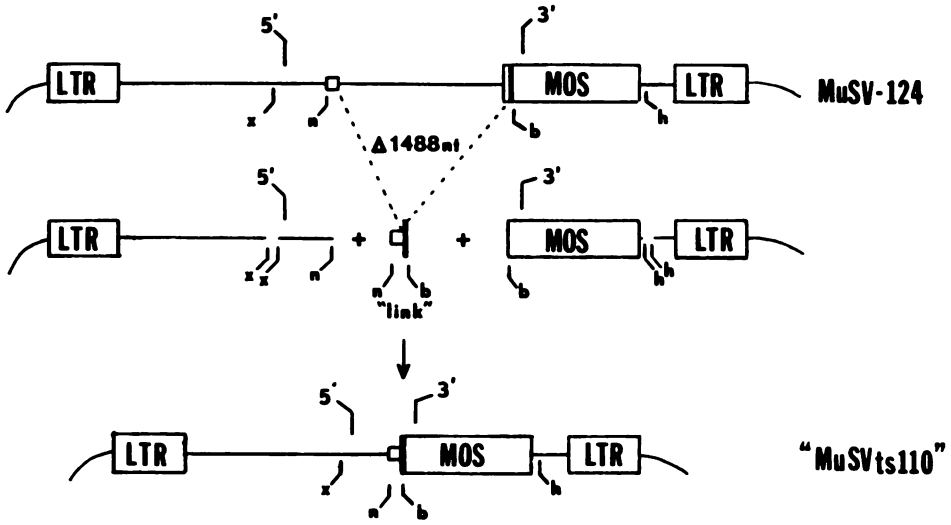

FIG. 5. Construction of MuSVts110 equivalent DNA. With wild-type MuSV-124 DNA as starting material, a 5'-splice-site fragment (*Xho*I [x] to *Nci*I [n]) and a 3'-splice-site fragment (*Bst*NI [b] to *Hin*dIII [h]) were ligated to a 70-base synthetic oligonucleotide (designated "link") composed of the sequence between the *Nci*I and *Bst*NI sites (2351 and 2421) in the MuSVts110 DNA. This fragment was subcloned and joined to wild-type viral DNA from which the original *Xho*I-to-*Hin*dIII fragment had been removed.

cleavage and exon ligation do not necessarily occur simultaneously during splicing of an individual pre-mRNA.

Analysis of abortive viral RNA splicing in a MuSVts110 revertant lacking part of the 3' splice site. In 6m2 cultures, revertants to the transformed state arise spontaneously at 39°C (2, 3). Two revertant cell lines, designated 54-5A4 and 204-3, have been studied (3, 32). We recently established that there is a 5-base deletion (-AGTGT-) at the usual 3' splice site in the MuSVts110 viral DNA in 54-5A4 cells (5). This deletion prevents splicing at this site but aligns the *gag* and *mos* genes into a continuous open reading frame, allowing the translation of transforming P100$^{gag\text{-}mos}$ from the unspliced RNA at any growth temperature (5, 32). To investigate the effect that loss of the AG dinucleotide might have on splicing reactions in vivo other than accurate exon ligation at the usual 3' splice site, we examined 5'-splice-site cleavage of viral RNA in 54-5A4 cells grown at various temperatures. We found that 5'-splice-site cleavage could be observed, but only at growth temperatures that normally would be permissive for MuSVts110 splicing (i.e., 33°C and lower) (Fig. 10). Substantial cleavage at the 5' splice site (25 to 30% of the viral transcripts) was observed at 28 and 33°C (Fig. 10, lanes 3 and 4; Table 2), but was markedly diminished (1 to 5%) at 35 to 41°C (Fig. 10, lanes 5 to 8; Table 2). In other pre-mRNAs in which the AG dinucleotide at the usual 3' splice site is altered, cryptic 3' splice sites are frequently activated in vivo (1). However, novel 3' splice sites were not activated by the mutation in the 54-5A4 viral RNA, although there is evidence for increased efficiency of an alternate splice event. S1 analysis of 54-5A4 RNA with

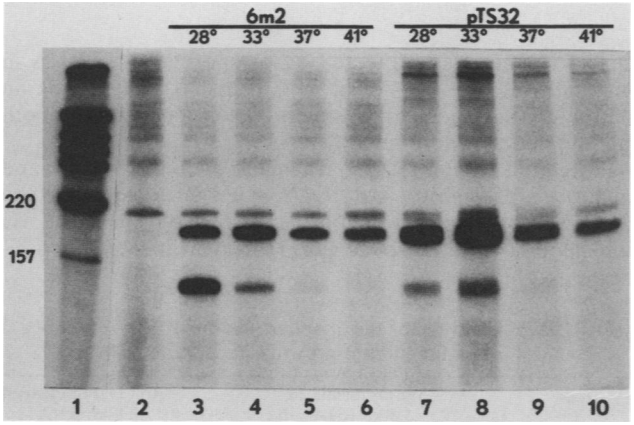

FIG. 6. Splicing of RNA transcribed from the MuSVts110 equivalent DNA. NIH 3T3 cells were cotransfected with the MuSVts110 equivalent DNA (designated pts32 DNA) and pSV2neo DNA. G-418-resistant colonies (here designated pTS32) were selected. RNA was prepared from 3T3/ts32 and control 6m2 cells grown at 28 to 41°C and subjected to S1 nuclease analysis with the pBA.36 probe as described in the legend to Fig. 2. Lanes 3 to 10 show protection of pBA.36 by RNA from control 6m2 or 3T3/ts32 cells, respectively, grown at 28°C (lanes 3 and 7), 33°C (lanes 4 and 8), 37°C (lanes 5 and 9), and 41°C (lanes 6 and 10). Lane 1, pBR322-*Hin*fI standard; lane 2, probe-only control.

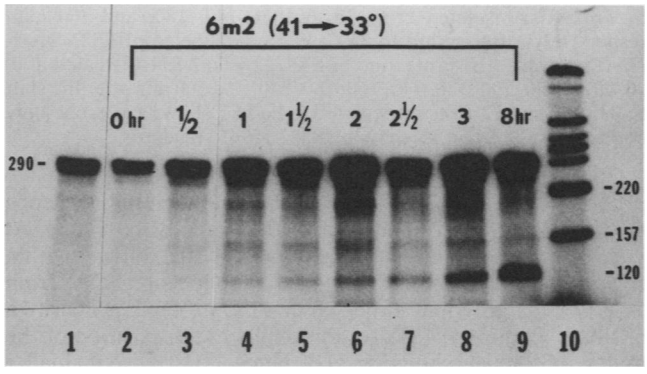

FIG. 7. Kinetics of 5'-splice-site cleavage in MuSVts110 viral RNA. Total 6m2 cellular RNA was isolated at various time intervals after a temperature shift from 41 to 33°C. RNA (10 μg) was subjected to S1 nuclease analysis with the 3'-end-labeled DD.29 probe (Fig. 1). The digestion products were analyzed on a 5% polyacrylamide gel containing 8 M urea. Lanes: 1, DD.29 probe; 2 to 9, protection of DD.29 by 6m2 cellular RNA isolated at 0, 30, 60, 90, 120, 150, 180, and 480 min, respectively, after the shift to 33°C; 10, pBR322 DNA-*Hin*fI standard.

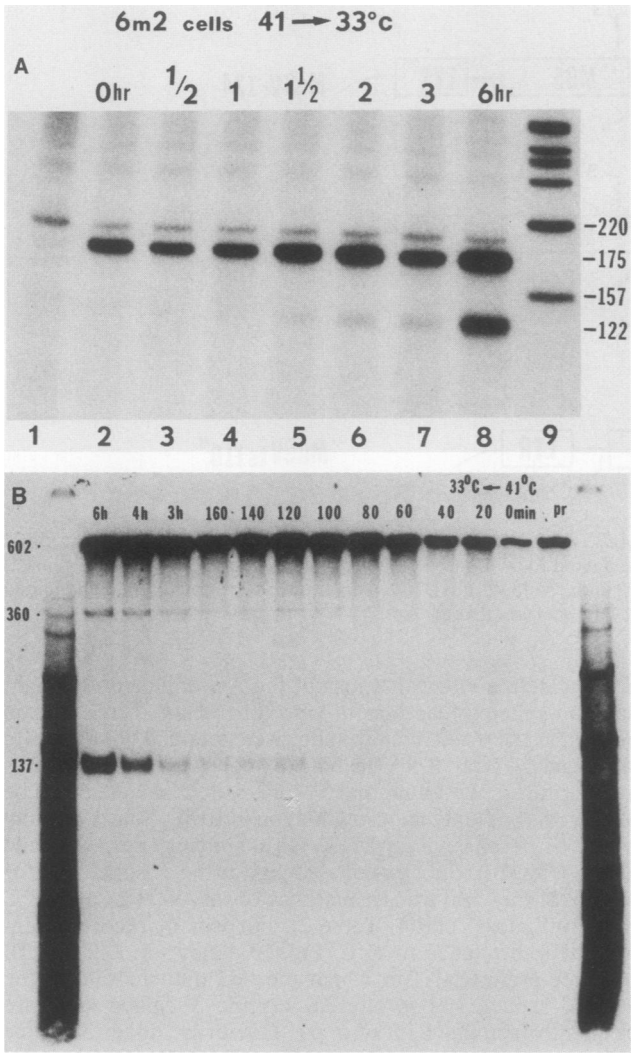

FIG. 8. Accumulation of ligated MuSVts110 exons. Total 6m2 cellular RNA was isolated at various time points after a temperature shift from 41 to 33°C and subjected to S1 nuclease analysis with the 5'-end-labeled pBA.36 (panel A) or 5'-end-labeled SX1.1 (panel B) probe. (A) lanes: 1, probe-only digest; 2 to 8, protection of pBA.36 by 6m2 RNA isolated at 0, 30, 60, 90, 120, 180, and 360 min, respectively, after a shift to 33°C; 9, 5'-end-labeled pBR322 DNA-*Hin*fI standard. (B) Protection of SX1.1 by 6m2 RNA isolated at 0, 20, 40, 60, 80, 100, 120, 140, 160, 180, 240, and 360 min after the shift to 33°C (lanes 3 to 14, respectively). Lane 2 shows the probe-only control. Lanes 1 and 15 show pBR322-*Hin*fI standards.

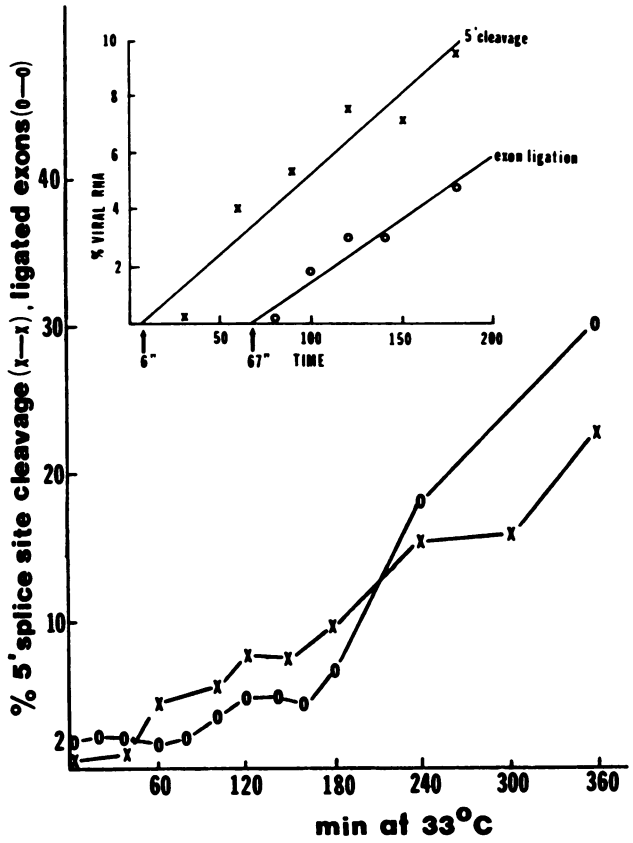

FIG. 9. Quantitation of splicing intermediates. Quantitative estimates of the levels of cleaved 5' splice sites (×) and ligated exons (○) as a function of time after a shift to 33°C were obtained by scanning each of the gel lanes shown in Fig. 7, 8A, and 8B. The levels of S1 nuclease protection fragments representing these RNA species were plotted as a percentage of the total viral RNA at each time point. The inset shows regression analysis of the 30- to 180-min time points in Fig. 7 (lanes 3 to 8) (×) and the 80- to 180-min time points in Fig. 8B (○).

probes (SX1.1, BB.220, and XN.369) that map the sequence to the right and left of the mutated 3' splice site (Fig. 11A) yielded no evidence for activation of cryptic splicing within several hundred bases of the usual 3' splice site. RNA from 54-5A4 cells grown at either 28 or 41°C protects primarily a 137-base fragment of SX1.1 that maps to the position of the mutated 3' splice site (Fig. 11B, lanes 3 and 4). No smaller protection fragments, indicative of recruitment of downstream cryptic 3' splice sites within the v-*mos* sequence, were detected. Using other probes, we have since shown that no cryptic splicing occurs within 444 bases downstream of the mutated 3' splice site in 54-5A4 viral RNA (S. M. Chiocca and E. C. Murphy, Jr., unpublished observations). However, an approximately 360-base fragment of SX1.1 was protected by 54-5A4 RNA at 28°C (Fig. 11B, lane 3). The same fragment was protected by the normal viral RNA in 6m2 cells at 33°C but not at 39°C (Fig. 8B), suggesting an alternate thermodependent splicing event occurring in both the mutated and normal viral RNAs.

Protection of this SX1.1 fragment by both normal and mutated MuSVts110 viral RNA at 33°C argues that the alternate splice site was not activated by the lost AG dinucleotide at the 3' splice site. However, it seemed possi-

TABLE 2. Cleavage of the 5' splice site in 54-5A4 viral RNA as a function of growth temperature

Temp (°C)	Amt of unspliced 3.8-kb RNA[a]	Amt (%) of cleaved 3.8-kb RNA[a]
28	15.4	7.3 (32)
33	20.7	6.7 (24)
35	19.7	2.7 (12)
37	14.2	0.8 (5.5)
39	10.9	0.6 (5.0)
41	12.7	0.1 (1.0)

[a] The degree of 5'-splice-site cleavage was estimated by scanning the gel profile shown in Fig. 11. The proportions of unspliced and cleaved 3.8-kb RNA were estimated from the levels of 290-base and 120-base DD.29 protection fragments, respectively, and expressed in arbitrary units.

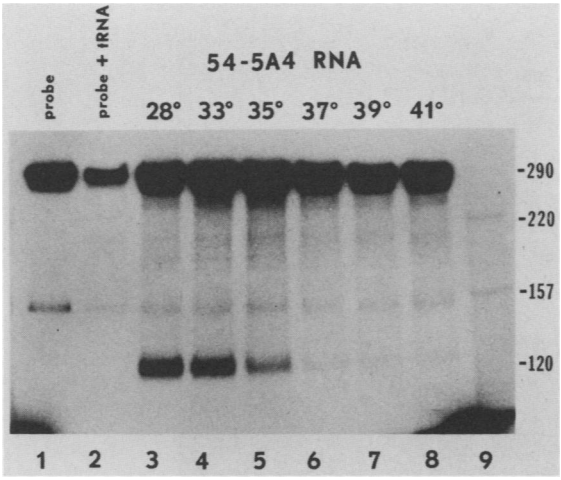

FIG. 10. Cleavage of the 5′ splice site in viral RNA in revertant 54-5A4 cells. Total cellular RNA (10 μg) from 54-5A4 cells grown at 28 to 41°C was hybridized to the 3′-end-labeled DD.29 probe. The hybrids were digested with S1 nuclease, and the fragments were analyzed on a 5% polyacrylamide gel containing 8 M urea. Lanes: 1, DD.29 probe-only control; 2, DD.29 probe plus yeast tRNA only; 3 to 8, protection of DD.29 by 54-5A4 RNA isolated at 28, 33, 35, 37, 39, and 41°C, respectively; 9, pBR322 DNA-*Hin*fI standard.

ble that the alternate splicing might be increased in efficiency in mutated 54-5A4 viral RNA. Thus, we used two other probes (BB.220 and XN.369 [Fig. 11A]) to map this and any other alternate splice sites within the MuSVts110 intron. Since there are no AG dinucleotides in the 26 bases between the downstream terminus of BB.220 and the MuSVts110 3′ splice site, we were confident that this probe could map any activation of splice sites within the intron. RNA from both 54-5A4 and control 6m2 cells grown at 39°C protected the expected 220- and 369-base fragments of BB.220 and XN.369, respectively, indicative of unspliced MuSVts110 RNA (Fig. 11C and D, all lanes). RNA from these 54-5A4 cells grown at 28°C, however, protected significant levels of both a 110-base XN.369 fragment (Fig. 11C, lane 5) and a 175-base BB.220 fragment (Fig. 11D, lane 3), mapping to either nucleotide 2239 or nucleotide 2240 of the MuSVts110 sequence, respectively. There is a good 3′ splice site consensus sequence in this region at nucleotide 2241 (-TCTTT CATTTGGCAG/TCT-). Splicing between this site and the MuSVts110 5′ splice site, however, would place a TAG and two TAA termination codons in the new frame between 60 and 100 bases downstream of the 3′ splice site. Thus, no *mos*-containing protein could be translated from such mRNA.

Quantitative estimates of the efficiency with which the alternate 3′ splice site is used in 6m2 versus 54-5A4 cells were made (Table 3). In 6m2 cells at 33°C, the alternate 3′ splice site was used at about one-fourth the efficiency of the usual 3′ splice site (8% versus 28%; data taken from quantitation of the Fig. 8B gel profile). In 54-5A4 cells, there was a significantly increased splicing at this site (to approximately 30%) that was presumably driven by a high concentration of 5′-cleaved splicing intermediates unable to splice at the usual 3′ splice site. Taken together, these data suggest that under conditions in which 54-5A4 viral RNA is cleaved at the 5′ splice site, no new cryptic 3′ splices are activated within 206 bases upstream and 137 bases downstream of the mutated 3′ splice site. However, our data indicate that an alternate 3′ splice site near nucleotide 2242, normally inefficiently used in 6m2 viral RNA, is used with increased efficiency.

DISCUSSION

The development of nuclear extracts capable of accurate pre-mRNA splicing in vitro has allowed several steps in this process to be outlined. Nascent pre-mRNAs first enter a multicomponent splicing complex and then undergo a series of cleavage and ligation reactions. In the first of these reactions, cleavage at the 5′ splice site and formation of a branched splicing intermediate occur virtually simultaneously. In the second step, the exons are ligated and a branched form of the intron is released (for reviews, see references 7 and 25). Analyses of the accuracy and efficiency of splicing of mutated pre-mRNAs with defined deletions and base substitutions have been of great utility in defining the critical sequences and interactions involved in the splicing process (1, 18, 24, 33, 37). In the work described in this report, we exploited the conditionally defective MuSVts110 retrovirus to study splicing events as they occur in vivo. As outlined, MuSVts110 is a novel mutant in which expression of the v-*mos* gene is governed by a conditional defect in viral RNA splicing (10, 11, 22, 23) that is in some way specified by the structure of the viral transcript. The potential to control the splicing of the MuSVts110 transcript by growth temperature shifts affords us a tractable system with which to study RNA splicing in vivo.

As we have shown here and elsewhere (2, 22, 23), accumulation of the spliced MuSVts110 3.3-kb RNA is restricted to growth temperatures of 33°C or lower. This restriction appears to be MuSVts110 RNA specific, since splicing of helper MuLV RNA in the same cells is not growth temperature restricted. MuLV RNA was chosen as a control because we expected it to be processed similarly to MuSVts110 RNA. (The transcriptional start sites and polyadenylation signals are identical, and the RNAs are virtually colinear through nucleotide 2404 and after nucleotide 3512 of the MuSVts110 sequence.) Consideration was also given to the fact that retroviral RNAs are differentially spliced, although the mechanism is poorly understood. Sufficient full-length viral RNA must be produced to serve as mRNA for the *gag* and *pol* gene products and to be packaged into virions, and sufficient splicing must occur to produce mRNA for the *env* gene products. Furthermore, 387 bases (nucleo-

TABLE 3. Alternate splicing of MuSVts110 RNA mutated at the 3′ splice site

Probe	Temp (°C)	6m2 viral RNA		54-5A4 viral RNA	
		3.8-kb + 3.3-kb	Alt[a] (% Alt)	3.8-kb	Alt[a] (% Alt)
SX1.1	33	92.3	7.4 (8.0)	ND	ND
	39	ND[b]	ND	ND	ND
BB.220	33	0.16	–[c]	0.29	0.20 (40)
	39	0.13	–	0.50	0.06 (12)
XN.369	33	0.30	–	0.79	0.43 (35)
	39	0.33	–	0.67	–

[a] The efficiency of alternate splicing (Alt) between the MuSVts110 5′ splice site at nucleotide 2017 and an alternate 3′ splice site near nucleotide 2242 was estimated by quantitation of the gel profiles shown in Fig. 8B (for 6m2 RNA with the SX1.1 probe) and in Figs. 11C and D. Amounts are expressed in arbitrary units.

[b] ND, Not done.

[c] –, Not measurable by scanning.

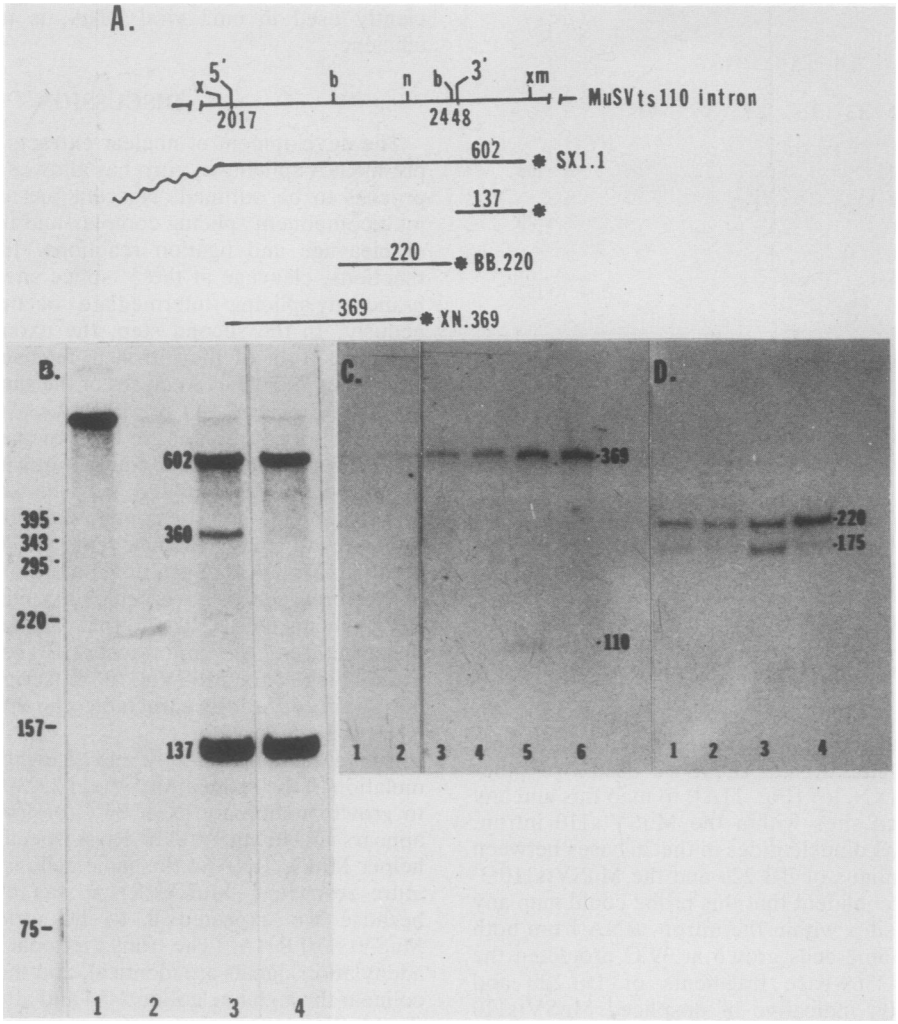

FIG. 11. S1 analysis of the MuSVts110 3′ splice site in 54-5A4 cells. (A) Total 54-5A4 cellular RNA was analyzed by S1 nuclease analysis with the 5′-end-labeled SX1.1, BB.220 and XN.369 probes. (B) Protection of SX1.1 DNA by RNA from 54-5A4 cells grown at 28°C (lane 3), (41°C) lane 4; lanes 1 and 2 represent SX1.1 probe alone and protection of SX1.1 by yeast tRNA, respectively. (C) Protection of XN.369 DNA by RNA from 54-5A4 cells grown at 28°C (lane 5) or 41°C (lane 6) and by RNA from 6m2 cells grown at 28°C (lane 3) or 41°C (lane 4). Lanes 1 and 2 represent protection of XN.369 by yeast tRNA and NRK RNA, respectively. (D) Protection of BB.220 by RNA from 54-5A4 cells grown at 28°C (lane 3) or 41°C (lane 4) and by RNA from 6m2 cells grown at 28°C (lane 1) or 41°C (lane 2).

tides 2017 to 2404) of the 431-base MuSVts110 intron encompasses a *gag* gene region that, if removed from MuLV, significantly inhibits *env* mRNA splicing (12). Given this level of complexity, we believed that the best control for specificity would be to monitor the splicing of another retroviral RNA at various growth temperatures. Since the splicing of MuLV RNA in 6m2 cells did not vary appreciably with growth temperature, the thermosensitive accumulation of the spliced MuSVts110 RNA was considered to be specific.

To address the possibility that splicing of MuSVts110 RNA occurs at all growth temperatures, but that the absence of the spliced RNA at 39°C reflects thermally driven selective degradation of RNA rather than inefficient splicing, we estimated the half-lives of both the unspliced and spliced viral RNAs at both 33 and 39°C. Our data showed that turnover of the spliced 3.3-kb RNA was doubled at 39°C ($T_{1/2}$, 4 h) over the 33°C rate ($T_{1/2}$, 9.7 h). However, this increase in turnover was not selective, since the turnover of the unspliced 3.8-kb RNA was also twice as fast under the same conditions ($T_{1/2}$ at 33°C, 18 h; $T_{1/2}$ at 39°C, 10 h). Thus, at 39°C the relative stabilities of the 3.8- and 3.3-kb RNAs were unchanged over those observed at 33°C, arguing that selective degradation of the 3.3-kb RNA at 39°C cannot explain the 10-fold difference in the relative levels of the spliced and unspliced RNAs (at 33°C the 3.3-kb/3.8-kb ratio was 0.24; at 39°C it was 0.026).

Further evidence of the heat stability of the 3.3-kb RNA can be inferred from previous studies on chronically superinfected 6m2 cells. In these cells, a viral RNA identical to the spliced 3.3-kb RNA and a P85$^{gag\text{-}mos}$ polypeptide are both observed at 39°C (8, 11). As might be predicted, these superinfected cells appear transformed at 39°C. Moreover, they contain a novel 3.35-kb MuSVts110-related viral DNA containing a deletion that maps in essentially the same place as the MuSVts110 intron (22), suggesting that a DNA copy of the spliced 3.3-kb MuSVts110 RNA was made by the reverse transcriptase of the helper MuLV and that this DNA can become integrated and transcribed. The constitutive transcription of the 3.3-kb RNA and expression of P85$^{gag\text{-}mos}$ at 39°C in these superinfected 6m2 cells strongly suggests that the 3.3-kb RNA is not intrinsically heat labile.

In 6m2 cells, temperature-sensitive viral RNA splicing seems to be an inherent property of the structure of the viral RNA. This was originally proposed as a result of experiments in which thermosensitive RNA splicing was retained in NRK cells infected with rescued MuSVts110 virions (10). In the current work, we have shown that transcripts derived from a MuSVts110 equivalent DNA introduced into NIH 3T3, Psi-2, or NRK cells can be spliced only at low growth temperatures. Thus, it seems plausible that the structure of the intron governs whether this RNA can successfully enter the splicing pathway. The arguments that support this reasoning are as follows. First, the wild-type parent of MuSVts110, MuSV-124, contains the same 5′ and 3′ splice sites used in MuSVts110. In MuSV-124, these splice sites are 1,919 bases apart and have never been observed to be spliced (E. C. Murphy, Jr., unpublished observations). Second, the MuSVts110 equivalent DNA contains only one change relative to wild-type MuSV-124: a 1,487-base deletion within the region between the cryptic splice sites. This deletion creates a 431-base intron that can be spliced at 33°C or lower. The deleted region is almost certainly composed exclusively of nonconserved intron sequences, since the sequence removed starts at 387 bases downstream of the 5′ splice site and ends 44 bases upstream of the 3′ splice site. However, since the branch point used in MuSVts110 RNA splicing has not yet been identified, we cannot exclude the possibility that the 1,487-base deletion activated a previously cryptic branch point. A clear inference from these observations is that the splice sites and probable branch point sequence in wild-type MuSV-124 are potentially competent but cryptic owing to some structural feature of the intervening sequence. Third, at least two other deletions between the cryptic splice sites in MuSV-124, one of 662 bases and another of 1,103 bases, will activate the viral transcript for temperature-sensitive splicing (M. de Mars, P. E. Cizdziel, and E. C. Murphy, Jr., manuscript in preparation). Taken together, these data strongly argue that the structural features of sequences intervening between competent splice sites can be crucial in determining splicing efficiency.

Since MuSVts110 pre-mRNA can be synchronized with respect to splicing, we were able to characterize some of the cleavage and ligation events in this process as they occur in vivo. Following a shift to 33°C, there was a short delay before cleavage at the 5′ splice site could be detected. The duration of this lag period is uncertain; intermediates cleaved at the 5′ splice site could first be detected between 30 and 60 min following the shift. However, analysis of the kinetics of the accumulation of these cleaved intermediates suggested that the first cleavage reactions could have occurred at about 6 min following the shift. Although the time taken for the cells to equilibrate to 33°C is an important but unknown variable in determining the actual length of the lag period, we favor the interpretation that the discrepancy between the 6-min and 30- to 60-min estimates for the lag period is a reflection of the time between the probable occurrence of the first cleavage events and the time at which intermediates cleaved at the 5′ splice site had accumulated sufficiently to be detected. A lag period of similar duration (about 15 to 45 min) (25) is also characteristic of splicing in vitro; during this time the pre-mRNA and various components of the splicing apparatus (e.g., small nuclear ribonucleoproteins [UsnRNPs]) are assembled into spliceosomes (18, 24).

Current evidence suggests strongly that branched RNA species containing the 5′-terminal guanosine of the cleaved intron linked 2′-5′ to an adenosine within 50 nucleotides of the 3′ splice site are intermediates in the splicing of eucaryotic pre-mRNAs (6, 14, 17, 18, 25, 29). These branch points present effective blockades to cDNA extension (29). However, we have not been able to identify the branch point nucleotide used in vivo in MuSVts110-infected cells shifted to 33°C. With primers complementary to sequences downstream of the 5′ and 3′ splice sites, as well as a primer that bridged the spliced exons, the only blockades to primer extension found mapped in either the intron or *gag* exon at all growth temperatures (P. E. Cizdziel and E. C. Murphy, Jr., unpublished results). No novel blockades to primer extension have yet been identified in the intron at temperatures permissive for splicing. It is apparent that the branched intermediate will have to be identified by the analysis of MuSVts110 RNA splicing in vitro.

Although there is evidence that 5′-splice-site cleavage and branch point formation may be individual aspects of a coupled reaction (26, 29), it is likely that exon ligation, the second step in the splicing process, is not necessarily coupled to 5′-splice-site cleavage. Our kinetic data indicate that exon ligation in individual MuSVts110 pre-mRNAs may be completed as late as 60 min after cleavage at the 5′ splice site.

Studies on splicing of viral RNA in the revertant 54-5A4 cell line in which the MuSVts2110 DNA lacks the sequence -AG/TGT- at the 3′ splice site have yielded some interesting results. Cleavage at the 5′ splice site can occur in the revertant viral RNA transcript without recruitment of a cryptic 3′ splice site within several hundred nucleotides of the usual 3′ splice site. However, an alternate 3′ splice site located at about the midpoint of the MuSVts110 intron and active in both 54-5A4 and 6m2 viral RNA at low temperatures was identified. In 6m2 cells, this splice site was used at about one-quarter the frequency of the usual 3′ splice site. In 54-5A4 cells, however, this alternate 3′ splice site appeared to be used much more efficiently; increased utilization is presumably driven by a high concentration of cleaved intron-exon 2 intermediates that cannot complete ligation at the usual 3′ splice site. Previous reports on the effect of alterations of the AG dinucleotide at the 3′ splice suggest that in in vitro splicing extracts, mutations of this kind allow cleavage at the 5′ splice site without the activation of cryptic 3′ splice sites, arguing that 5′-splice-site cleavage and exon ligation can be uncoupled (27, 28, 30). In vivo, however, there is good evidence that mutations in the AG dinucleotide lead to the activation of cryptic 3′ splice sites, frequently at the closest downstream AG dinucleotide (1). In the MuSVts110 revertants mutated at the 3′ splice site, this pattern of cryptic splice-site activation does not occur. There are eight AG dinucleotides between the mutated 3′ splice site and the 5′ end of the SX1.1 probe. None of these possible sites, however, were activated for splicing. Instead, there appeared to be an increased utilization of an alternate 3′ splice site, already being used at low efficiency in normal MuSVts110 transcripts and relatively far upstream (206 nucleotides) of the usual 3′ splice site. It seems very likely that an increased utilization of an alternate 3′ splice site in a pre-mRNA mutated at the usual 3′ site is a plausible alternative to activation of a cryptic site.

At 39°C in 6m2 cells no splicing intermediates can be detected, although it has been shown that MuSVts110 3.8-kb RNA can associate with some spliceosome components at this temperature, as evidenced by its immunoprecipitation with anti-Sm and anti-(U1) ribonucleoprotein sera (9). It is not known whether these viral RNA-spliceosome component complexes are inactive because they are incomplete or

whether the structure assumed by the MuSVts110 transcripts prevents the initiation of splicing. However, there is a delay of no more than 30 to 60 min duration between the shift to 33°C and the first appearance of MuSVts110 transcripts cleaved at the 5′ splice site. Since this lag period is very similar to that observed after the addition of presynthesized pre-mRNA to in vitro splicing extracts, our data suggest that the inactive MuSVts110 RNA-containing complexes can become active after a shift to 33°C. However, since not all of the MuSVts110 pre-mRNA in cells at 39°C is associated with spliceosome components (9), the possibility cannot be excluded that these inactive complexes remain inactive and only newly synthesized viral RNA and any preexisting viral RNA not in association with spliceosome components at 39°C are the source of spliced viral RNA.

As yet, the biochemical basis for the temperature sensitivity of the splicing event is not known. However, since viral mutants exhibiting temperature-sensitive splicing can be generated from the splicing-inactive MuSV-124 virus by a variety of deletions corresponding to nonconserved intron sequences between the 5′ and 3′ splice sites used in the MuSVts110 mutant (de Mars et al., in preparation), it seems most likely that this splice event is specified by intron sequences. Moreover, alternate viral RNA splicing in the revertant 54-5A4 cell line provides another clue. In the revertant 54-5A4 cell line, splicing of the alternate 225-base intron (extending between nucleotides 2017 and 2242 and corresponding to the 5′ half of the 431-base MuSVts110 intron) occurred only at growth temperatures that would be permissive for splicing of the normal MuSVts110 RNA (i.e., containing an intact 3′ splice site at nucleotide 2448). Thermosensitive splicing of this alternate intron suggests that sequences at the 5′ end of the usual MuSVts110 intron may specify temperature-sensitive splicing.

ACKNOWLEDGMENTS

We are indebted to Michele M. Herrick, Jade L. Wong, and James J. Syrewicz for their excellent technical assistance. The assistance of Nancy Edwards in manuscript typing and editing, Tania Busch in photography, and Ron La Biche in calculating mRNA half-lives is greatly appreciated.

This work was supported in part by grants from the National Cancer Institute (Public Health Service grant CA34734) and the Robert A. Welch Foundation (grant G-894) and by National Cancer Institute Core Grant CA16672 support for the University of Texas System Cancer Center Macromolecular Synthesis Facility. Paul E. Cizdziel and Maryellen de Mars are supported by Rosalie B. Hite Predoctoral Fellowships.

LITERATURE CITED

1. **Aebi, M., H. Hornig, R. Padgett, J. Reiser, and C. Weissman.** 1986. Sequence requirements for splicing of higher eukaryotic nuclear pre-mRNA. Cell **47**:555–565.
2. **Biggart, N., G. Gallick, and E. C. Murphy.** 1987. Nickel-induced heritable alterations in retroviral transforming gene expression. J. Virol. **61**:2378–2388.
3. **Blair, D., M. Hull, and E. Finch.** 1979. The isolation and preliminary characterization of temperature-sensitive transformation mutants of Moloney murine sarcoma virus. Virology **95**:303–316.
4. **Brown, D., J. Horn, L. Wible, R. B. Arlinghaus, and B. Brinkley.** 1981. Analyses of the sequence of events in the transformation process in cells infected with a temperature sensitive transformation mutant of Moloney murine sarcoma virus. Proc. Natl. Acad. Sci. USA **78**:5593–5597.
5. **Cizdziel, P., M. Nash, D. Blair, and E. C. Murphy.** 1986. Molecular basis underlying phenotypic revertants of Moloney murine sarcoma virus MuSVts110. J. Virol. **57**:310–317.
6. **Grabowski, P., R. Padgett, and P. Sharp.** 1984. Messenger RNA splicing in vitro: an excised intervening sequence and a potential intermediate. Cell **37**:415–427.
7. **Green, M. R.** 1986. Pre-mRNA splicing. Annu. Rev. Genet. **20**:671–708.
8. **Hamelin, R., B. Brizzard, M. Nash, E. C. Murphy, and R. B. Arlinghaus.** 1985. Temperature-sensitive viral RNA expression in Moloney murine sarcoma virus *ts*110-infected cells. J. Virol. **53**:616–623.
9. **Hamelin, R., E. Chan, E. Tan, and R. B. Arlinghaus.** 1986. Antibodies against small nuclear ribonuclearproteins immunoprecipitate complexes containing ts110 Moloney murine sarcoma virus genomic and messenger RNAs. Virology **152**:87–99.
10. **Hamelin, R., K. Kabat, D. Blair, and R. B. Arlinghaus.** 1986. Temperature-sensitive splicing defect of *ts*110 Moloney murine sarcoma virus is virus encoded. J. Virol. **57**:301–309.
11. **Horn, J., T. Wood, E. C. Murphy, D. Blair, and R. B. Arlinghaus.** 1981. A selective temperature sensitive defect in viral RNA expression in cells infected with a ts transformation mutant of murine sarcoma virus. Cell **25**:37–46.
12. **Huang, L.-H. S., J. Park, and E. Gilboa.** 1984. Role of intron-contained sequences in formation of Moloney murine leukemia virus RNA. Mol. Cell. Biol. **4**:2289–2297.
13. **Junghans, R., E. C. Murphy, and R. B. Arlinghaus.** 1982. Electron microscopic analysis of ts110 Moloney mouse sarcoma virus, a variant of wild-type virus with two RNAs containing large deletions. J. Mol. Biol. **161**:229–255.
14. **Keller, W.** 1984. The RNA lariat: a new ring to the splicing of mRNA precursors. Cell **39**:423–425.
15. **Kloetzer, W., S. Maxwell, and R. B. Arlinghaus.** 1983. $P85^{gag\text{-}mos}$ encoded by ts110 Moloney murine sarcoma virus has associated protein kinase activity. Proc. Natl. Acad. Sci. USA **80**:412–416.
16. **Kloetzer, W., S. Maxwell, and R. B. Arlinghaus.** 1984. Further characterization of the $P85^{gag\text{-}mos}$ associated protein kinase activity. Virology **138**:143–155.
17. **Konarska, M., P. Grabowski, R. Padgett, and P. Sharp.** 1985. Characterization of the branch site in lariat RNAs produced by splicing of mRNA precursors. Nature (London) **313**:552–557.
18. **Krainer, A., T. Maniatis, B. Ruskin, and M. Green.** 1984. Normal and mutant human beta-globin pre-mRNAs are faithfully and efficiently spliced in vitro. Cell **36**:993–1005.
19. **Lazo, P. A., V. Prasad, and P. N. Tsichlis.** 1987. Splice acceptor site for the *env* message of Moloney murine leukemia virus. J. Virol. **61**:2038–2041.
20. **Maniatis, T., and R. Reed.** 1987. The role of small nuclear ribonucleic protein particles in pre-mRNA splicing. Nature (London) **325**:673–678.
21. **Mann, R., and D. Baltimore.** 1985. Varying the position of a retrovirus packaging sequence results in the encapsidation of both spliced and unspliced RNAs. J. Virol. **54**:401–407.
22. **Nash, M., B. Brizzard, J. Wong, and E. C. Murphy.** 1985. Murine sarcoma virus *ts*110 RNA transcripts: origin from a single proviral DNA and sequence of the *gag/mos* junctions in both precursor and spliced viral RNAs. J. Virol. **53**:624–633.
23. **Nash, M., N. Brown, J. Wong, R. B. Arlinghaus, and E. C. Murphy.** 1984. S1 nuclease mapping of viral RNAs from a temperature-sensitive transformation mutant of murine sarcoma virus. J. Virol. **50**:478–488.
24. **Newman, A., R.-J. Lin, S.-C. Cheng, and J. Abelson.** 1985. Molecular consequences of specific intron mutations on yeast mRNA splicing in vivo and in vitro. Cell **42**:335–344.
25. **Padgett, R., P. Grabowski, M. Konarska, S. Seiler, and P. Sharp.** 1986. Splicing of messenger RNA precursors. Annu. Rev. Biochem. **55**:1119–1150.
26. **Padgett, R. A., M. Konarska, P. J. Grabowski, S. F. Hardy, and P. Sharp.** 1984. Lariat RNAs as intermediates and products in the splicing of mRNA precursors. Science **225**:898–903.
27. **Reed, R., and T. Maniatis.** 1985. Intron sequences involved in lariat formation during pre-mRNA splicing. Cell **41**:95–105.
28. **Ruskin, B., and M. Green.** 1985. Role of 3′ splice site consensus sequence in mammalian pre-mRNA splicing. Nature (London) **317**:732–734.
29. **Ruskin, B., A. Krainer, T. Maniatis, and M. Green.** 1984.

Excision of an intact intron as a novel lariat structure during pre-mRNA splicing in vitro. Cell **38**:317–331.
30. **Rymond, B., and M. Rosbash.** 1985. Cleavage of 5′ splice site and lariat formation are independent of 3′ splice site in yeast mRNA splicing. Nature (London) **317**:735–737.
31. **Shinnick, T., R. Lerner, and J. Sutcliffe.** 1981. Nucleotide sequence of Moloney murine leukemia virus. Nature (London) **293**:543–548.
32. **Stanker, L., J. Horn, G. Gallick, W. Kloetzer, E. C. Murphy, D. Blair, and R. B. Arlinghaus.** 1983. gag-mos polyproteins encoded by variants of the Moloney strain of mouse sarcoma virus. Virology **126**:336–347.
33. **Treisman, R., S. Orkin, and T. Maniatis.** 1983. Specific transcription and RNA splicing defects of five cloned beta-thallasemia genes. Nature (London) **302**:591–596.
34. **Van Beveren, C., F. van Straaten, J. Galleshaw, and I. Verma.** 1981. Nucleotide sequence of the genome of a murine sarcoma virus. Cell **27**:97–108.
35. **Zeitlin, S., and A. Efstratiadis.** 1984. In vivo splicing products of the rabbit beta-globin pre-mRNA. Cell **39**:589–602.
36. **Zeitlin, S., A. Parent, S. Silverstein, and A. Efstratiadis.** 1987. Pre-mRNA splicing and the nuclear matrix. Mol. Cell. Biol. **7**:111–120.
37. **Zhuang, Y., and A. M. Weiner.** 1986. A compensatory base change in U1 snRNA suppresses a 5′ splice site mutation. Cell **46**:827–835.